Effects of Galvanic Coupling between Carbon Steel and Stainless Steel Reinforcement in Concrete

Luca Bertolini, Matteo Gastaldi, MariaPia Pedeferri and Pietro Pedeferri
Dipartimento di Chimica Fisica Applicata del Politecnico di Milano
piazza L. da Vinci 32, 20133 Milan, Italy

Tommaso Pastore
Facoltà di Ingegneria, Università degli Studi di Bergamo,
via G. Marconi, 5 - 24044 Dalmine, Italy

ABSTRACT

The behaviour of stainless steel coupled with carbon steel is evaluated in order to study the consequences of galvanic coupling on corrosion of reinforced concrete structures where stainless steels bars are used for limited parts of the reinforcement. The paper reports the results of measurements of free corrosion potential, corrosion rate and macrocouple current in reinforced concrete specimens, as a function of chloride contamination and humidity. The cathodic behaviour of stainless steel and carbon steel is studied by means of potentiostatic and potentiodynamic tests in alkaline solutions. The results show that the galvanic coupling with stainless steel can enhance the corrosion rate of active carbon steel reinforcement in carbonated or chloride contaminated concrete, but this increase is appreciable only under particular situations. In any case it is not worse than the coupling with passive carbon steel.

Keywords: reinforced concrete, stainless steel, corrosion, macrocouple, galvanic coupling.

INTRODUCTION

Corrosion of steel in chloride-contaminated or carbonated concrete can be avoided by using corrosion-resistant alloys instead of carbon steel. Stainless steels have been used for complete or partial substitution of carbon steel in new structures exposed to aggressive environments or when a very long service life is required. They have also been used in the repair of reinforced concrete structures damaged by corrosion (especially for historic building restoration), in order to guarantee long-term effectiveness of the repair work.

In the past years, there has been considerable development in the chemical composition of stainless steels, in their physical and mechanical properties, and in the types of reinforcement available (plain or ribbed bars as well as welded mesh). Furthermore, it was shown that, depending on the chemical composition and microstructure (austenitic, ferritic, martensitic or duplex), a suitable type of stainless steel for environments from mild to very aggressive can be found.[1-11]

Use of stainless steels is limited by their higher cost compared with carbon steel (7 to 12 times higher). However, a more realistic comparison should be done on the basis of the life-cycle cost of the structure, i.e., also taking into consideration future costs

related to repair and maintenance of the reinforced concrete structures through the service lives. In that case the use of stainless steel in aggressive environments or in constructions with very long service life appears much more attractive.

Concern has been expressed with regard to the risk of galvanic corrosion when stainless steel is used in partial substitution of carbon steel. In fact, if stainless steel is electrically connected with carbon steel, galvanic corrosion could be induced on carbon steel.

This work deals with the effect of galvanic coupling between stainless steel and carbon steel in chloride-contaminated structures. Galvanic coupling tests were carried out on concrete specimens. The macrocouple current which arised by connecting corroding carbon steel with passive stainless steel was compared with that brought about by passive carbon steel, in order to clarify whether the use of stainless steel in new structures or in the repair of corroding structures might have harmful consequences. The cathodic behaviour of stainless steels and carbon steel was studied by means of electrochemical tests in alkaline solutions. To study the influence of oxide scale produced by welding on the surface of stainless steel, tests were also carried out on stainless steel bars subjected to high temperature oxidation.

EXPERIMENT

Macrocouple tests have been carried out on carbon steel and 316L stainless steel of the composition reported in Table 1 in concrete. Concrete was mixed with 350 kg/m^3 of portland cement, 0.5 w/c ratio, 1900 kg/m^3 of limestone aggregate, and addition of a superplasticizer. Both concrete without chlorides and concrete with 3% chloride by cement weight, added as $CaCl_2$ in the mixing water, were used. Concrete was cured for 28 days in a wet environment.

Two parallel bars were embedded in reinforced concrete specimens of dimension 20×20×5 cm. Three types of specimens were obtained (Figure 1, specimens A_1, A_2 and A_3). They had a bar of carbon steel embedded in concrete with 3% Cl^-, while the other bar was respectively: *a*) carbon steel in chloride free concrete, *b*) AISI 316L stainless steel in chloride-free concrete, *c*) AISI 316L stainless steel in 3% Cl^- concrete. Activated titanium reference electrodes were fixed in the middle of each bar for measuring the steel potential. The ends of the bars were coated with a heat shrinkable sleeve, so that only a length of 15 cm was exposed to the concrete.

After curing, the specimens were exposed to 95-98% R.H. at 25°C. Free corrosion potential and corrosion rate were monitored for 10 days. Corrosion rate was measured with the linear polarization technique by imposing a potential scan rate of 10 mV/minute in the range ±10 mV with respect to the free corrosion potential. Corrosion rate (i_{cor}) was evaluated by means of Stern-Geary relationship: $i_{cor}=C/R_p$ where R_p is polarization resistance (obtained from potential/current density curves) and C was assumed equal to 26 mV.

After the electrical connection of the two bars of each specimen by means of an external wire, potential of the bars and macrocouple current density were monitored. In order to report potential values versus the saturated calomel reference electrode (SCE), before macrocouple tests the potential of the activated titanium electrodes was verified versus an external reference electrode placed on the surface of the concrete. The macrocouple current was measured as ohmic drop on a 100 Ω shunt and was expressed as current density with respect to the area of the exposed surface of the corroding

rebar. The relative humidity of the environment was maintained at 95-98% for 15 days and then reduced to 65-75%.

A test was also carried out on specimen *B* of dimensions 20×20×10 cm, showed in Figure 1, where the corroding bar of carbon steel was connected simultaneously with a bar of passive carbon steel and a bar of AISI 316L stainless steel in chloride-free concrete. The contributions to the macrocouple current due to the carbon steel and the stainless steel bars were measured separately.

Cathodic polarization tests were carried out in saturated $Ca(OH)_2$ (pH 12.6) and 0.9M NaOH (pH 13.9) alkaline solutions at 25°C. Cylindrical specimens of diameter 1 cm and height 20 mm were exposed to the solution for at least 48 hours before testing. The surface of the specimens was finished with 1200 mesh emery paper. Potentiodynamic tests were carried out with a scan rate of 20 mV/min from the free corrosion potential. Potentiostatic polarization tests were carried out at potentials ranging from -300 to -600 mV vs SCE for 24 hour. These tests were also carried out on AISI 304L stainless steel.

Cathodic polarization tests were also carried out on specimens left for ten minutes at temperatures of 300, 500, 700 or 900°C, so that oxides of different colours were produced on their surface depending on the temperature. Macrocouple tests with concrete specimens of Figure 1*a* were carried out by using stainless steel bars treated at 700°C.

RESULTS

Figure 2 shows the average value of the potential and the corrosion rate of carbon steel and AISI 316L stainless steel during the exposure in free corrosion conditions at 95-98% R.H. before of galvanic coupling. Free corrosion potential of carbon steel in concrete with 3% of chloride by cement weight was around -400 mV vs SCE, and corrosion rate was 10-20 mA/m^2. Free corrosion potential of passive steels (i.e., carbon steel in chloride free concrete or AISI 316L stainless steel) ranged between -200 and -50 mV vs SCE, while corrosion rate was of the order of 0.1 mA/m^2. More positive value of the corrosion potential and slightly higher corrosion rates (although still absolutely negligible) were measured on the stainless steel with oxide scale produced at 700°C.

Figure 3 shows, as an example, the potential of the bars and the macrocouple current density during the first minute after the connection of corroding carbon steel and AISI 316L stainless steel embedded in concrete with 3% chloride. Following the electrical connection of the two bars, macrocouple current flows from the corroding carbon steel bar in 3% Cl^- concrete (anode) to the passive bar (cathode). The current density decreases from an initial value of about 100 mA/m^2 to a value lower than 10 mA/m^2 within a minute. Changes in potential are mainly confined to the passive stainless steel which shows a decrease from above -100 mV vs SCE to below -400 mV vs SCE. Conversely, potential of corroding carbon steel shows only a slight increase. After the first minute of coupling, changes in potential and macrocouple current density are much slower.

Figures 4 and 5 show the potentials and the macrocouple current density during all the duration of the tests on specimens with different types of passive bar (specimens of Figure 1*a*). Changes in potential and macrocouple current density occur soon after the coupling (as it has already been observed with the example of Figure 3), while rather stable values were measured during the 15 days at R.H. of 95-98%. When R.H. was

decreased to 65-75%, so that concrete could get drier, the potential of the coupled rebars showed a progressive change towards less negative values and the macrocouple current density decreased.

Comparison of Figure 4 with Figure 5 evidences that the macrocouple current brought about by a passive bar of carbon steel is 5-7 times higher than the current induced by passive bar of stainless steel.

Figure 6 shows the results of the test where the corroding carbon steel bar in concrete with 3% chloride was connected simultaneously to two passive bars of carbon steel and stainless steel in chloride free concrete (specimen *B* of Fig. 1). Even in this case it is clearly evident that, although the free corrosion potential of stainless steel is rather similar to that of passive carbon steel and thus the driving voltage for the macrocouple is also similar, the macroucouple current generated by the AISI 316L stainless steel is much lower than that of passive carbon steel.

Figure 7 shows the results of the macrocouple tests with rebars of AISI 316L stainless steel with an oxide scale produced at 700°C. By comparing this figure with Figure 5 it can be observed that the macrocouple current is almost one order of magnitude higher on the passive stainless bars with the oxide scale.

The cathodic polarization curves of carbon steel and AISI 316L stainless steel in alkaline solutions are showed in Figure 8. Both results of potentiodynamic polarization tests (Figure 8*a*) and 24 hour potentiostatic polarization tests (Figure 8*b*) are reported. Both types of test show a different cathodic behaviour for the stainless steel compared with carbon steel. It can be observed that in the range of potential between -300 and -600 mV vs SCE the polarization curve of AISI 316L stainless steel is below the curve of carbon steel. This means that stainless steel has higher cathodic overvoltages and thus, when it is cathodically polarized, for a given potential it leads to a lower cathodic current density. The increase in pH from 12.6 to 13.9 decreased the cathodic overvoltage on both materials; however the curve of stainless steel remained below that of carbon steel (Figure 8*a*).

Figure 9 shows the cathodic potentiodynamic polarization curves of AISI 316L stainless steel covered by oxide scale produced at temperatures from 300 to 900°C. The oxide scale, especially that produced at temperatures above 300°C, reduces the cathodic overvoltages, both at pH 12.6 (Figure 9*a*) and at pH 13.9 (Figure 9*b*). Curves of the stainless steel with oxide scale are even above the curve of carbon steel. The higher current densities were obtained with specimens treated at 700°C.

The increase in pH from 12.6 to 13.9 seems not to affect the curves of the stainless steel in the presence of oxide scales.

Figure 10 shows polarization curves of AISI 304L stainless steel, which are very similar to those of AISI 316L stainless steel.

DISCUSSION

In reinforced concrete structures a macrocouple can arise between bars electrically connected which show appreciable differences in the free corrosion potentials (i.e. the potentials measured before the connection). The macrocouple current can flow through concrete from the steel with the more negative potential (acting as anode) to that with the more positive value (cathode). Such a current stimulates corrosion on the anode.

Galvanic coupling usually occurs in reinforced concrete structures also without stainless steels. For instance a macrocouple can form when only a part of the reinforcement (e.g., the less deep mat) is depassivated. The still passive bars act as

cathodes and the corroding bars act as anodes, and thus corrosion rate can be enhanced in the latter. Nevertheless, the increase in corrosion rate due to this galvanic coupling is usually modest, and it becomes appreciable only if the cathode surface is much higher than the anode surface, depending on geometry and on concrete resistivity.[12]

Since the passive film on stainless steels is much more stable than that of carbon steel, and thus they can be passive in a wider range of conditions, they can influence the galvanic coupling phenomena which can occur in reinforced concrete structures where they are used together with carbon steel.

When both carbon steel and stainless steel reinforcements are passive and in aerated concrete, the macrocouple usually does not produce appreciable effects, since the two types of steel have almost the same free corrosion potential (Figure 2). Indeed, in this environment, normally carbon steel is slightly more noble than stainless steel. In particular, both carbon steel and stainless steel remain passive even after connection. A significant macrocouple can only arise under very particular conditions. For example, when highly chloride-contaminated and non-aerated (i.e., water saturated) concrete is confined around stainless steel (in this condition pitting corrosion does not take place on stainless steel even for very high chloride concentration) whereas, elsewhere, aerated conditions persist on passive carbon steel connected with the stainless steel, the risk of pitting initiation on stainless steel is similar to that in aerated conditions.

Conversely, when the carbon steel is already corroding, the macrocouple current is significant. Figure 10*a* shows the stable values of the macrocouple current density during the tests at 95-98% R.H. It can be observed that the coupling of AISI 316L stainless steel with the carbon steel bar in 3% chloride concrete, which had a corrosion rate before coupling of around 15 mA/m^2 (Figure 2), lead to a macrocouple current density of (1.5 to 2.5) mA/m^2. This means that coupling with stainless steel brought about a negligible increase in the corrosion rate of carbon steel in chloride contaminated concrete (about 10%). It should be observed that both geometrical condition (two parallel bars) and exposure conditions (high humidity) were such to maximize macrocouple effects.

Furthermore, Figure 10*a* also shows that, environmental conditions and geometry being the same, passive carbon steel lead to a much higher macrocouple current density of 10 mA/m^2. Therefore, the increase in corrosion rate on carbon steel embedded in chloride-contaminated concrete due to galvanic coupling with stainless steel was significantly lower than the increase induced by coupling with passive carbon steel. Similar result were obtained with a relative humidity of 65-75% (Figure 10*b*), although owing to the higher resistivity of concrete the macrocouple current was smaller.

The lower macrocouple current density for stainless steel compared to passive carbon steel is a consequence of its cathodic behaviour. Figure 8 shows that in alkaline solution higher overvoltage for the cathodic reaction of oxygen reduction was found on stainless steel with respect to carbon steel.

The high cathodic overvoltage on stainless steel means that when stainless steel is polarized to a negative potential owing to galvanic coupling with corroding carbon steel (for instance at potential values lower than -400 mV SCE as shown in Figure 3), it can produce a current density several times lower than the current density that passive carbon steel can generate. Thus the consequence of coupling with stainless steel is generally negligible since passive areas of carbon steel always surround the area where corrosion takes place. If only stainless steel brought about an exceptional increase in the cathode to anode area ratio, it would lead to significant consequences.

As a consequence of these findings, stainless steel has even to be considered a better reinforcement material for use in repair projects when a part of the corroded reinforcement is to be replaced compared with usual carbon steel. Because of being a poor cathode, the stainless steel will minimise eventual problems which could occur in neighbouring corroding and passive areas after the repair.

Nevertheless, tests on bars with high temperature oxide scale showed a worse behaviour for stainless steel. In fact, oxide scale produced at high temperature lead to a significant decrease in the cathodic overvoltage (Figures 8 and 9). The macrocouple current density generated by stainless steels with oxide scale was of the same order of magnitude or even higher than that produced by coupling with carbon steel (Figure 11). Consequently, oxide scale produced by welding (as well as mill scale) on stainless steel bars that is not removed can locally stimulate corrosion on carbon steel (although extension of areas wit welding scale is usually rather small).

CONCLUSIONS

The coupling of corroding carbon steel with stainless steels are generally modest, and they are negligible with respect those due to the coupling with passive carbon steel which always surround the corroding area.

The increase in corrosion rate on carbon steel embedded in chloride-contaminated concrete due to galvanic coupling with stainless steel is significantly lower than the increase brought about by coupling with passive carbon steel, since stainless steel has higher overvoltage for the cathodic reaction of oxygen reduction with respect to carbon steel.

Low overvoltage, similar to that observed on carbon steel, was observed on stainless steel with oxide scale formed at high temperature. The oxide scale increased the macrocouple current density generated by stainless steels to values of the same order of magnitude or even higher than that produced by coupling with carbon steel.

AKNOWLEDGEMENTS

The authors are grateful to Acciaierie Valbruna SpA for supporting this work.

REFERENCES

1. Smith, F.N., Cutler, C.P., Cochrane, D.J., "Stainless Steel Reinforcing Bars", *Proceedings.* International Conference on Understanding Corrosion Mechanisms of Metals in Concrete. A Key to Improving Infrastructure Durability, M.I.T., Cambridge (MA), 27-31 July 1997.
2. Nürnberger, U. (Ed.), "Stainless Steels in Concrete - State of the Art Report", European Fede. of Corrosion, Publ. N.18, The Inst. of Materials, London, 1997.
3. Brown, B.L., Harrop, D., Treadaway, K.W.J., "Corrosion Testing of Steels for Reinforced Concrete", Building Research Establishment, Garston, 45/78, 1978.
4. Treadaway, K.W.J., Cox, R.N., Brown, B.L., "Durability of Corrosion Resisting Steel in Concrete", *Proc. Instn. of Civil Engineers*, Part 1, 1989, pp. 305-331.
5. Sorensen, B., Jensen, P.B., Maahn, E., "The Corrosion Properties of Stainless Steel Reinforcement", *Corrosion of Reinforcement in Concrete* (ed. C.L. Page), Elsevier, London, 1990, pp. 601-605.

6. Callaghan, G., "The Use of 3Cr12 as Reinforcing in Concrete", *Corrosion Science*, Vol. 35, 1993, pp. 1535-1541.
7. Pastore, T., Pedeferri, P., Bertolini, L., Bolzoni, F., Cigada, A., "Electrochemical Study on the Use of Stainless Steels in Concrete", *Procedings*. Int. Conf. 'Duplex Stainless Steel 1991', Beaune, France, Vol. 2, 1991, pp. 905-913.
8. Nurnberger, U., Beul, W., Onuseit, G., "Corrosion Behaviour of Welded Stainless Reinforced Steels in Concrete", *Otto-Graf-Journal*, No. 4, 1993, pp. 225-259.
9. Bertolini, L., Bolzoni, F., Pastore, T., Pedeferri, P., "Stainless Steel Behaviour in Simulated Concrete Pore Solution", *British Corrosion Journal*, Vol.31, No. 3, 1996, pp. 218-222.
10. Pedeferri, P., Bertolini, L., Bolzoni, F., Pastore, T., "Behaviour of Stainless Steels in Concrete", *Proceedings, The State of the Art of the Repair and Rehabilitation of Reinforced Concrete Structures*", Maracaibo, 27 April- 1 May 1997.
11. Bertolini, L., Pedeferri, P., Pastore, T., "Stainless Steel in Reinforced Concrete Structures", *Proceedings*, Second Int. Conf. on Concrete under Severe Conditions, CONSEC/98, Tromsø, 21-24 June 1998.
12. Andrade, C., Gonzalez, S., Maribona, S.R., "Macrocell versus Microcell Corrosion of Reinforcements Placed in Parallel", CORROSION/92, NACE, Houston, May 1992, Paper No. 194.

Table 1 - Chemical composition of carbon steel and stainless steels.

Steel	C	Si	Mn	Cr	Ni	Mo	P	S	N	Al
Carbon steel	0.077	0.165	0.536	0.047	0.109	0.02	0.009	0.02	-	0.002
AISI 316L	0.017	0.45	1.54	16.47	10.86	2.04	0.029	0.027	0.05	-
AISI 304L	0.014	0.62	1.48	18.19	9.14	-	0.028	0.026	0.05	-

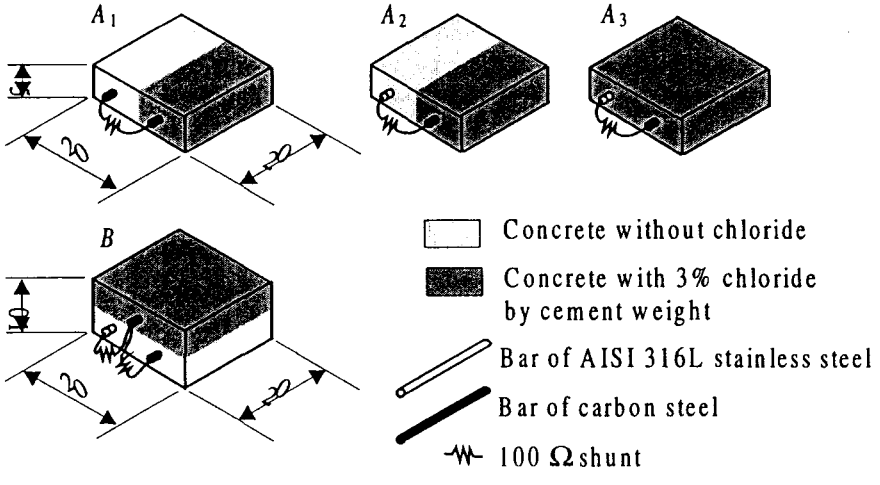

Figure 1 - Specimens used for galvanic coupling tests with connection of two rebars (A_1, A_2, A_3) and with connection of three rebars (B). Dimensions in cm.

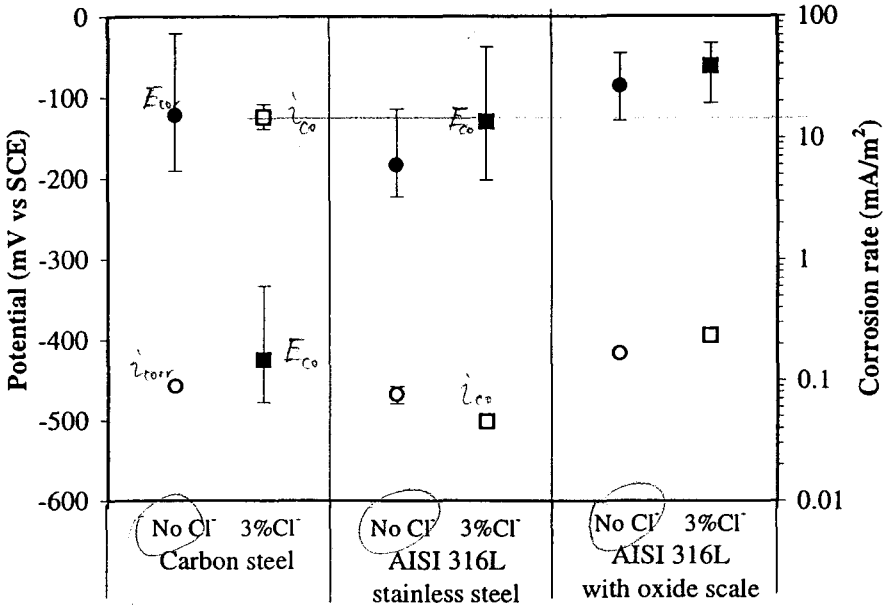

Figure 2 - Free corrosion potential and corrosion rate of carbon steel and AISI 316L stainless steel: free corrosion potential (●) and corrosion rate (○) in chloride free concrete; free corrosion potential (■) and corrosion rate (□) in concrete with 3% chloride by cement weight at 95-98% R.H. and 25°C.

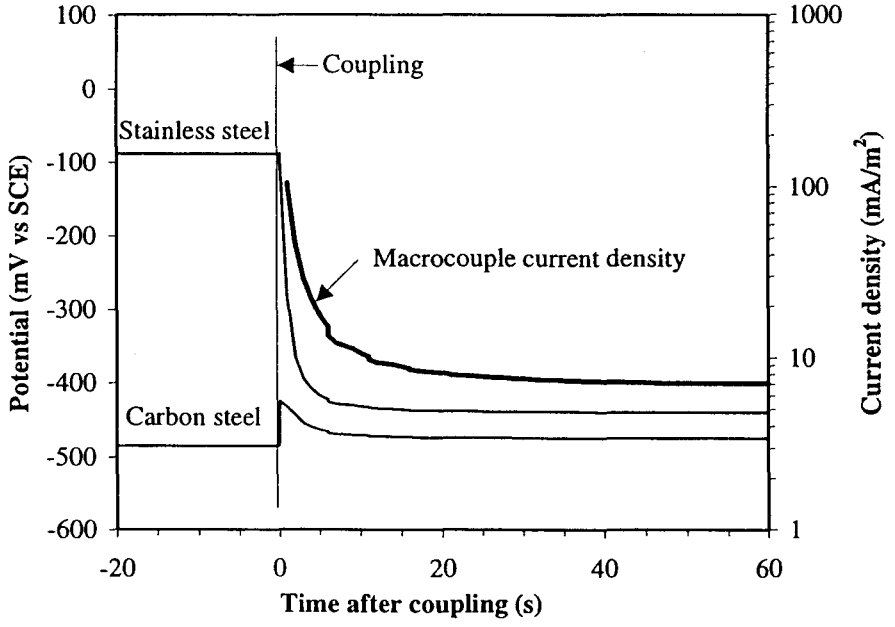

Figure 3 - Potential of carbon steel and AISI 316L stainless steel in concrete with 3% chloride by cement weight and macrocouple current density during the first minute of coupling (specimen type A_3).

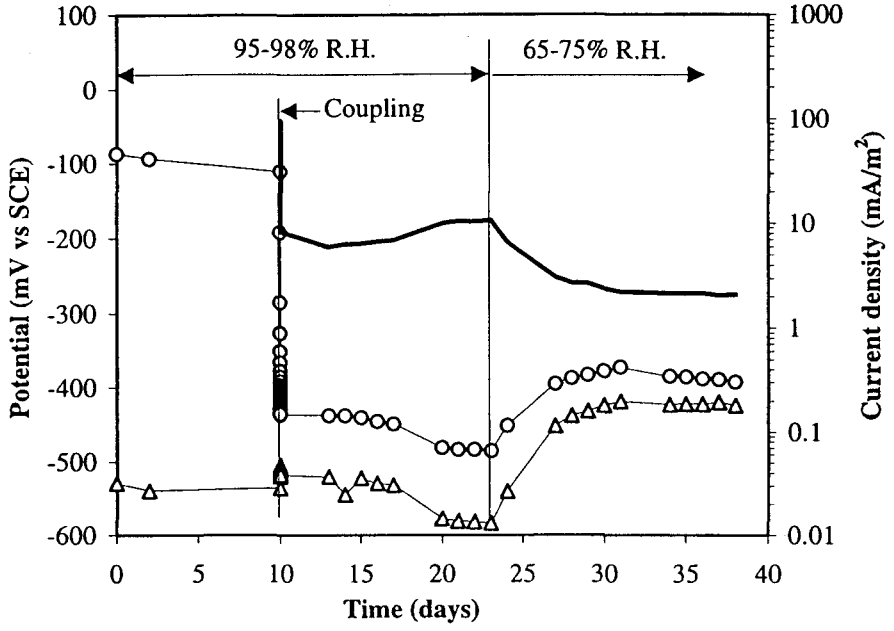

Figure 4 - Galvanic coupling between corroding carbon steel in concrete with 3% chloride by cement weight and carbon steel in chloride free concrete (specimen type A_1): potential of corroding carbon steel (Δ), potential of passive carbon steel (O) and macrocouple current density (——).

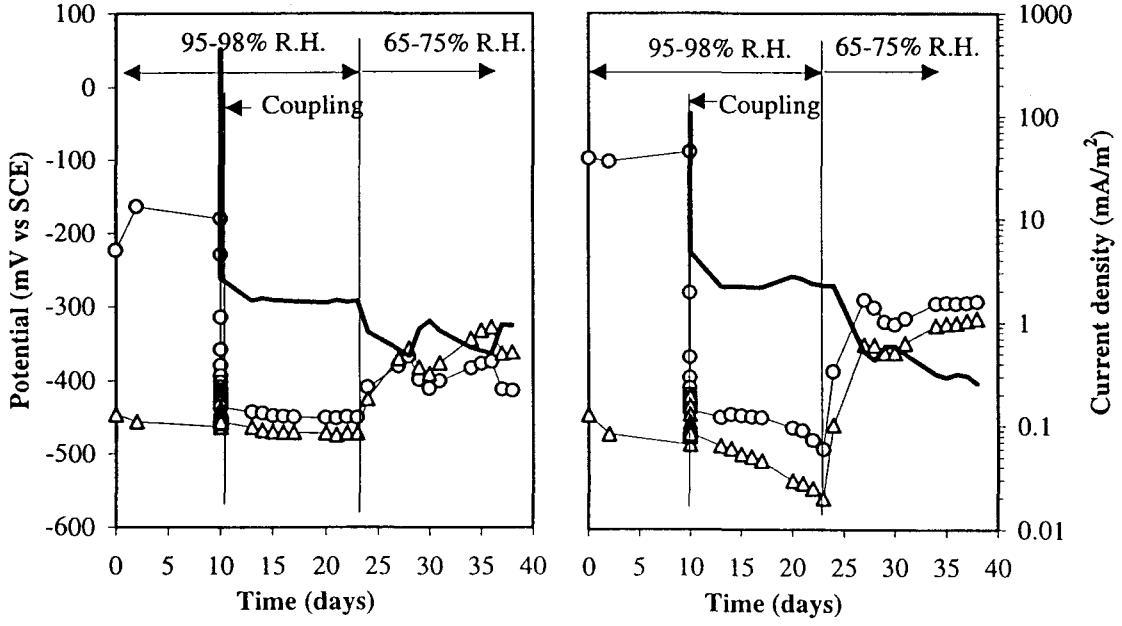

(*a*) (*b*)

Figure 5 - Galvanic coupling between corroding carbon steel in concrete with 3% chloride by cement weight and AISI 316L stainless steel in chloride free concrete (*a*, specimen type A_2) and in concrete with 3% chloride by cement weight (*b*, specimen A_3): potential of corroding carbon steel (Δ), potential of passive stainless steel (O) and macrocouple current density (——).

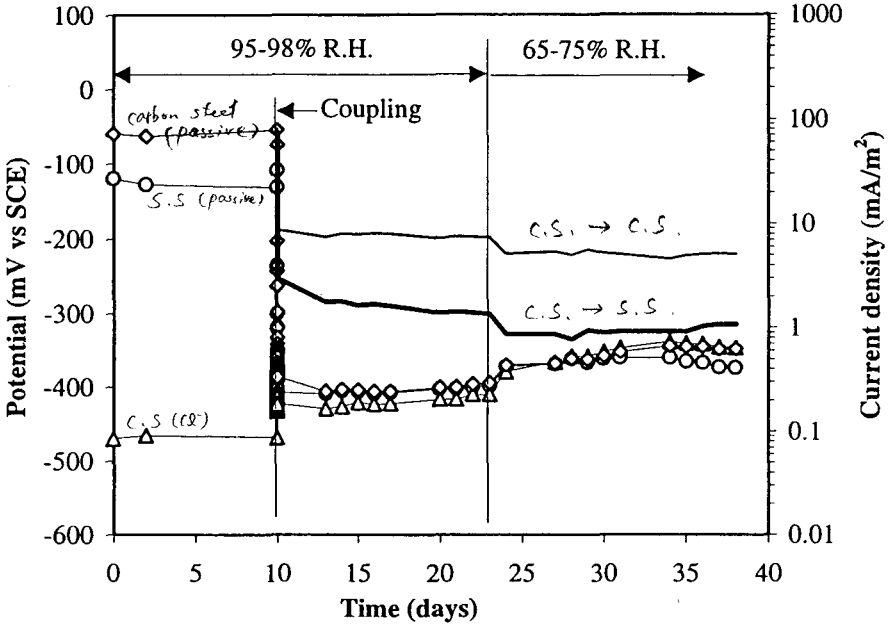

Figure 6 - Galvanic coupling between corroding carbon steel in concrete with 3% chloride by cement weight and passive carbon steel and AISI 316L stainless steel in chloride free concrete (specimen type *B*): potential of corroding carbon steel (Δ), potential of passive carbon steel (✧), potential of passive stainless steel (O); macrocouple current density between corroding and passive carbon steel (—), macrocouple current density between corroding carbon steel and stainless steel (——).

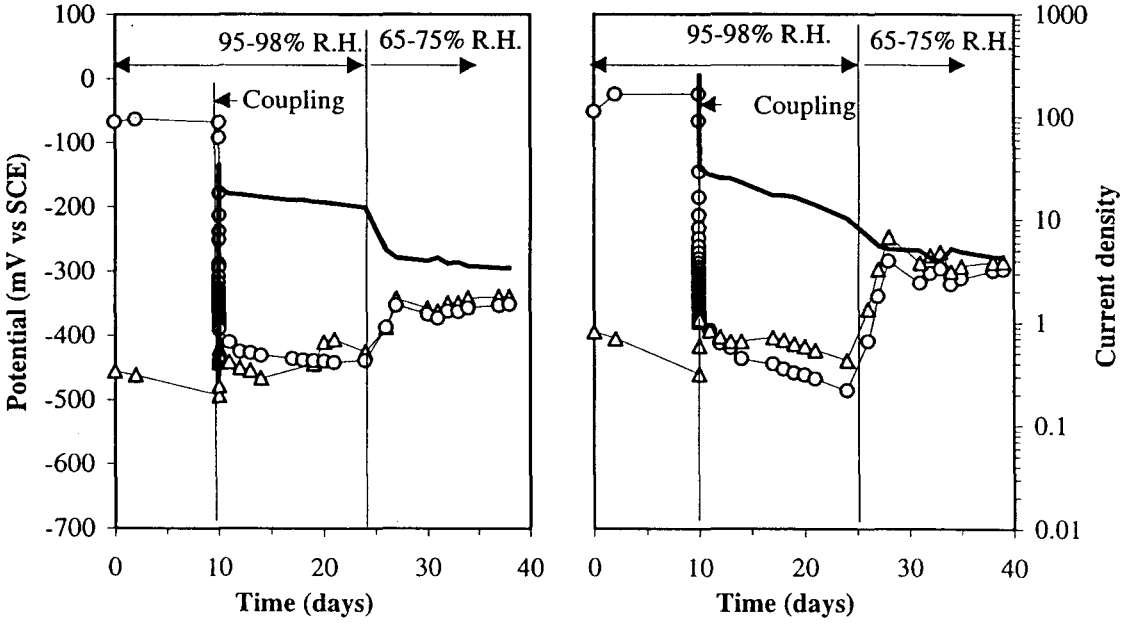

Figure 7 - Galvanic coupling between corroding carbon steel in concrete with 3% chloride by cement weight and AISI 316L stainless steel with oxide scale in chloride free concrete (*a*, specimen type A_2) and concrete with 3% chloride by cement weight (*b*, specimen type A_3): potential of corroding carbon steel (Δ), potential of passive stainless steel (O) and macrocouple current density (——).

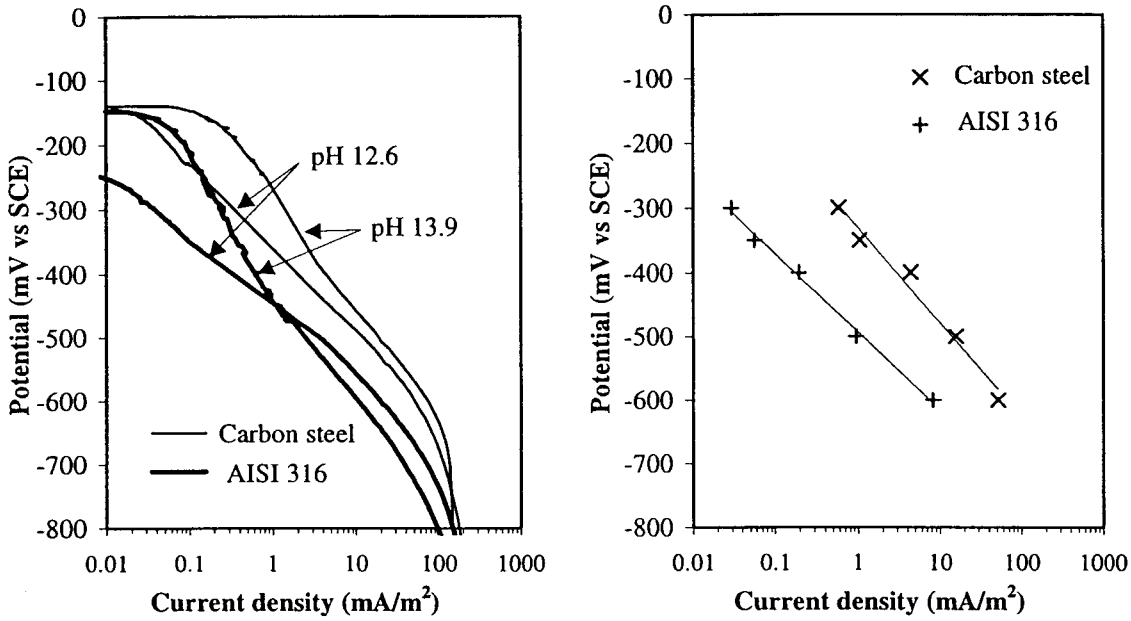

(*a*) (*b*)

Figure 8 - Cathodic polarization curves of carbon steel and AISI 316L stainless steel in saturated $Ca(OH)_2$ (pH 12.6) and 0.9M NaOH (pH 13.9) solutions, obtained with potentiodinamic polarization tests (*a*) and potentiostatic polarization tests (*b*).

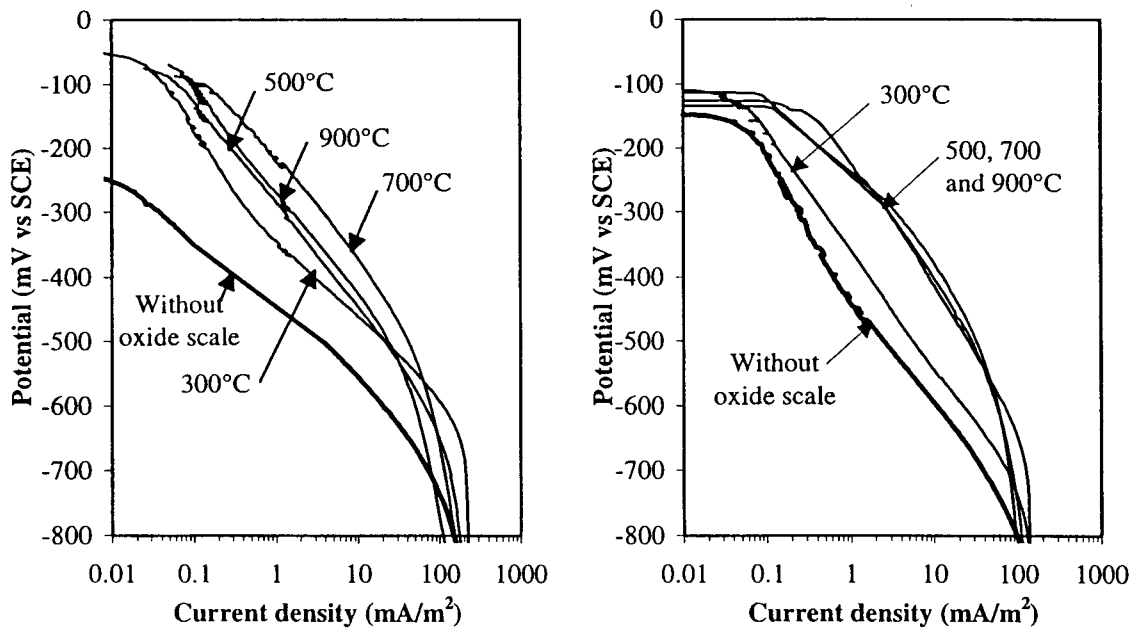

(*a*) (*b*)

Figure 9 - Influence of oxide scale produced at different temperatures on the cathodic polarization curve of AISI 316L stainless steel in saturated $Ca(OH)_2$ solution with pH 12.6 (*a*) and in the 0.9M NaOH solution with pH 13.9 (*b*).

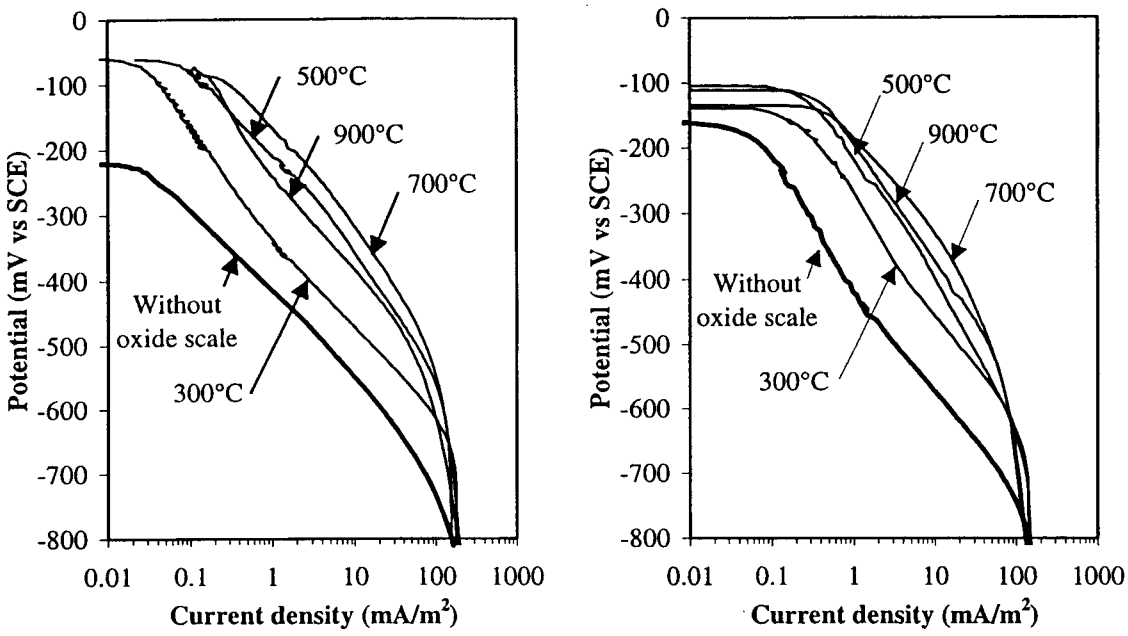

Figure 10 - Influence of oxide scale produced at different temperatures on the cathodic polarization curve of AISI 304L stainless steel in saturated $Ca(OH)_2$ solution with pH 12.6 (*a*) and in the 0.9M NaOH solution with pH 13.9 (*b*).

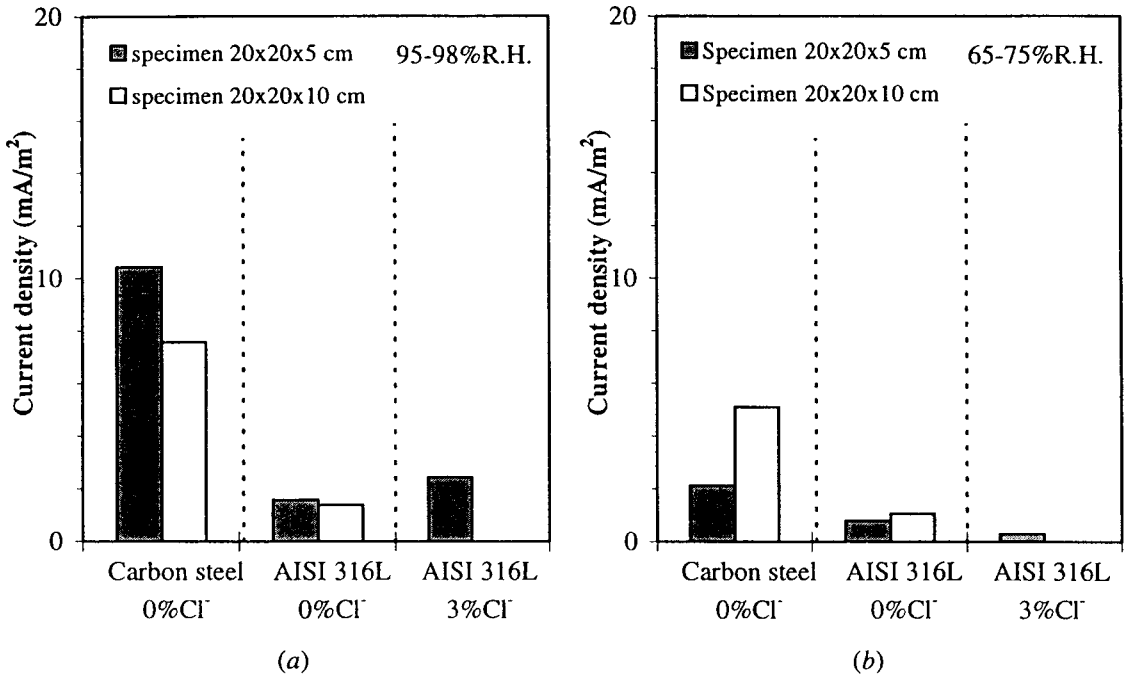

Figure 11 - Macrocouple current density exchanged between a corroding bar of carbon steel in 3% chloride contaminated concrete connected with a passive bar of: carbon steel in chloride free concrete,

AISI 316L in chloride free concrete or AISI 316L in 3% chloride contaminated concrete (average value of the macrocouple current density measured between 12 and 15 days of exposure at each R.H.).

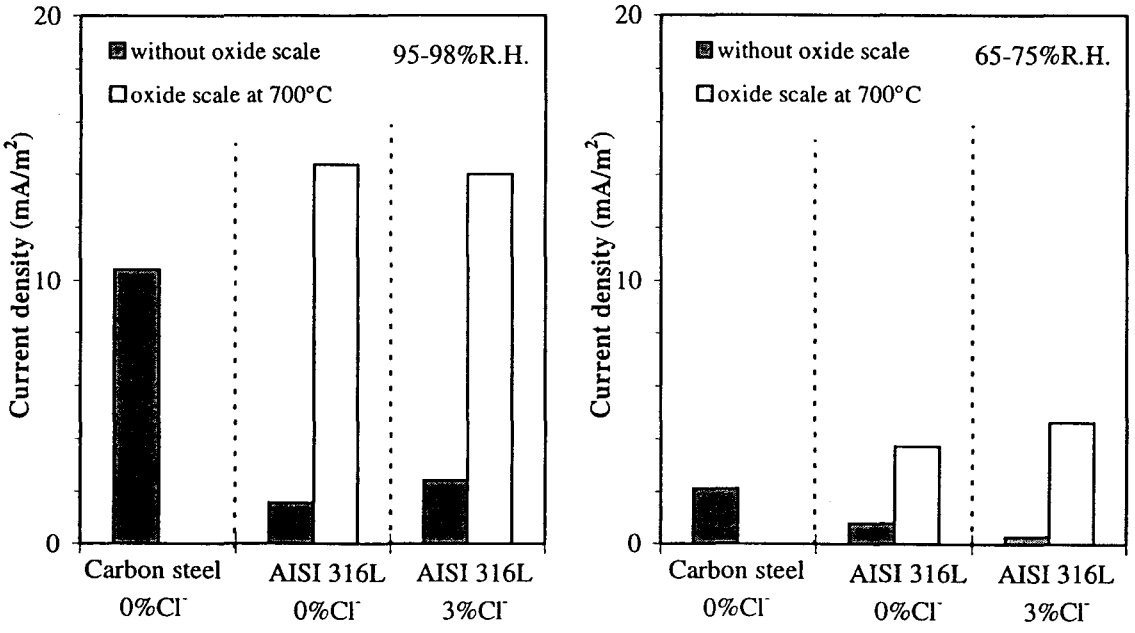

Figure 12 - Influence of oxide scale on the surface of AISI 316L stainless steel on the macrocouple current density exchanged with a corroding bar of carbon steel in 3% chloride contaminated concrete (average value of the macrocouple current density measured between 12 and 15 days of exposure at each R.H.).